Nuclear Instruments and Methods in Physics Research B 369 (2016) 34–39

Contents lists available at ScienceDirect

Nuclear Instruments and Methods in Physics Research B

journal homepage: www.elsevier.com/locate/nimb

Experimental study on the interference of autoionizing states of He

Béla Paripás *, Béla Palásthy, Miklós Béres

Institute of Physics, University of Miskolc, 3515 Miskolc-Egyetemváros, Hungary

ARTICLE INFO

Article history:
Received 7 July 2015
Received in revised form 21 October 2015
Accepted 22 October 2015
Available online 6 November 2015

Keywords:
Exchange interference
Argon
Constant-ionic-state $(e, 2e)$ experiment (CIS)

ABSTRACT

The interference of the low-lying doubly excited autoionizing states of helium ($2s^2(^1S)$, $2s2p(^3P)$, $2p^2(^1D)$ and $2s2p(^1P)$) is studied. In this paper we concentrate on the interference of the direct and indirect ionization ($He^+ 1s^{-1}$) in the neighborhood of the critical energy (93.15 eV) of the possible state-to-state interference of the $2s^2(^1S)$ and $2p^2(^1D)$ resonances. The spectra of autoionizing and scattered electrons measured in three angular ranges at around 87–97 eV primary energy are shown with the computer fitted parameters of the peaks.

1. Introduction

During the phenomenon of interference two or more waves superimpose and form a resultant wave of greater or lower amplitude. Interference usually refers to the interaction of coherent waves that originate from the same source, but travel via two different paths. These two paths in quantum mechanics can correspond to the two different ways through which the system forms a common final state from a common initial state. In a well-known case, the $F(E_F)$ final ionic state with energy E_F is formed either directly from the $G(0)$ initial (ground) atomic state Eq. (1a) or via an intermediate $R(E_R)$ resonance Eq. (1b).

$$G(0) + e^-(E_0) \rightarrow F(E_F) + e_s^-(E_s) + e_a^-(E_a) \tag{1a}$$

$$G(0) + e^-(E_0) \rightarrow R(E_R) + e_s^-(E_s) \rightarrow F(E_F) + e_s^-(E_s) + e_a^-(E_a) \tag{1b}$$

In both processes the primary electron e^- is inelastically scattered (e_s^-) and an electron (e_a^-) is also ejected. In case of the resonant two-step pathway Eq. (1b) both emitted electron energies are determined ($E_s = E_0 - E_R$, $E_a = E_R - E_F$) giving two peaks in the electron energy spectrum. In the direct process Eq. (1a) the two electrons in the final state share the excess energy ($E_0 - E_F$) in a continuous manner. A quantum mechanical interference that occurs between these two processes, i.e., between the resonant and the direct process is the so called Fano interference and it causes a well-known asymmetric distortion of spectral lines in the electron spectra.

There is another kind of interference that can modify the coincidence spectra. Suppose that a second non-overlapping resonance R' is also excited by electron impact on the atomic ground state G and it decays into the same final state by electron emission:

$$G(0) + e^-(E_0) \rightarrow R'(E_{R'}) + e_{s'}^-(E_{s'}) \rightarrow F(E_F) + e_{s'}^-(E_{s'}) + e_{a'}^-(E_{a'}) \tag{2a}$$

The interference condition requires that the energy (and spin) of the scattered electron from one reaction path equals the energy (and spin) of the ejected electron released along the other reaction path: in such case the electron pairs (e_s^-, e_a^-) and ($e_{s'}^-$, $e_{a'}^-$) are indistinguishable. Such exchange interference (i.e. between the two resonant pathways Eqs. (1b) and (2a)) therefore occurs only at unique electron impact energy: $E_0 = E_R + E_{R'} - E_F$.

The state-to-state exchange interference was first observed [1,2] in non-coincidence experiments, namely in the energy-loss spectra of helium autoionizing resonances. Since then several researchers have performed similar measurements with photon excitation, using other noble gas targets. These are summarized in article [3]. Earlier we made an effort [4] to experimentally demonstrate this interference in other systems: we studied the resonant Auger decay of the $[2p_{1/2}]4p$ and $[2p_{3/2}]4p$ resonances of argon that decay into the same final state $[3p^2](^1D_2)4p(^2P,^2D)$. Our experimental approach was based on CIS (constant ionic state) coincidence $(e, 2e)$ measurements. We isolated the final state by keeping the sum of the scattered electron energy and the Auger electron energy constant. This was achieved by scanning the transmission energies of the two spectrometers in the opposite direction during the measurement in such a way, so as to keep their sum constant. Although around the "critical" energy we found systematic differences as well, we did not find these

* Corresponding author.
E-mail address: fizpari@uni-miskolc.hu (B. Paripás).

http://dx.doi.org/10.1016/j.nimb.2015.10.044
0168-583X/

significant enough to state unambiguously the existence of interference effects. We concluded that the high density of states in the region of interest might smear out the effect.

Because of the above reasons we switched to the simplest possible target, helium. We concentrated the possible state-to-state interferences of the $2s^2(^1S)$ and $2p^2(^1D)$ autoionizing resonances (decaying to the same simple He^+1s^{-1} final state), and their possible interference that was studied at the very first in a different way [1,2]. Our goal was again to perform an experimental study of state-to-state interference by $(e,2e)$ CIS method where both electrons are detected in restricted angular ranges. We found that around the critical energy, a few tenths of eV modification in primary energy causes a significant change in the CIS spectra, which indicates the presence of exchange interference effects [5]. On the other hand, however, the measured CIS spectra could be reproduced only partly. We found at least two reasons of this long-term instability. First of all, the emissivity of the cathode changed after some months (or after an emergency stoppage), which resulted in a primary electron beam with a different cross-sectional distribution. This changed the angular dependence of the ratio of the yields corresponding to the different scattering angles. Secondly, we could not perform an accurate energy calibration for both the electron gun and the spectrometers without a computer fit of measured spectra. (We estimated a 0.1 eV calibration error for every element of the system.) The first uncertainty can be decreased by a further confinement of measuring angles, while the elaboration of a proper computer fit can solve the second problem. In this paper we show these improvements and the first results obtained by these new tools.

2. Experimental improvements

The spectrometer system used in this experiment has been described in detail previously [6], so only a brief description is given here. Basically, our measuring system consists of two cylindrical mirror (CMA) spectrometers on a common axis (Fig. 1). Each spectrometer consists of two "box" type analyser [7] stages. Because of the small room in the vacuum chamber, one of the four analysers had to be build shorter. For this reason, spectrometer B (containing the shorter analyser) has approx. 1.4 times weaker energy resolution than spectrometer A. We fitted 0.55% and 0.78% FWHM values for the peaks at around 200 eV (argon $[2p_{1/2,3/2}]4p$ resonances) and 0.80% and 1.10% FWHM values for the peaks at around 35 eV (this experiment) for A and B spectrometers, respectively. The common axis of the spectrometers is perpendicular to both the target gas beam and the projectile electron beam. These three perpendicular lines cross at the common focal point of the spectrometers.

The scattered or ejected electrons that enter the analysers and have appropriate energy pass the analysers and are detected by channel electron multipliers (CEM). The pulse counting of the

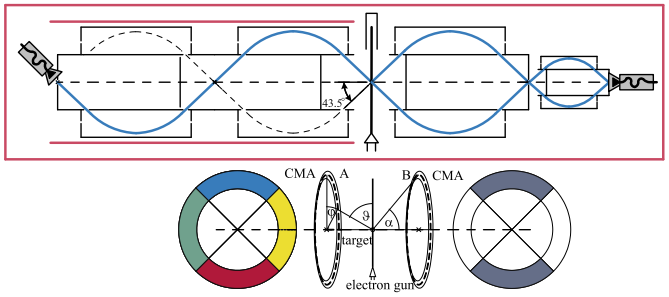

Fig. 1. The geometry of the scattering volume.

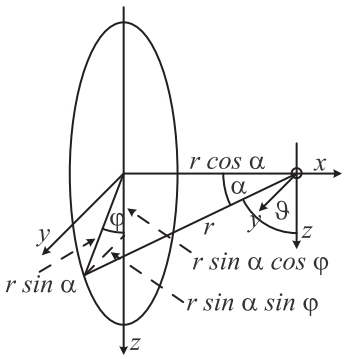

Fig. 2. The sketch and entrance geometry of our $(e,2e)$ coincidence spectrometer system.

amplified and shaped CEM signals, and the controlling of the analyser voltages are performed by measuring cards in a PC running the LabWindows program. The program is capable to control both spectrometers in the desired energy range, even in opposite scanning directions.

The nearly 5°-wide entrance cones in the CMA spectrometers provide large acceptance solid angles, which are essential in coincidence measurements. Since the entrance angle with respect to the CMA axis is close to $\alpha_0 = 43.5°$, the entrance angular range is $\alpha = 41–46°$. When the entrance cone was open all around ($\varphi = 360°$), the scattering angle (ϑ) of detected electrons relative to the primary electron beam fell into the range of 47—133°. The goal of the latest rebuilding was to limit the φ rotational angle of the spectrometer ($\Delta\varphi = 90°$) in such a way that the limited range can be rotated along the whole circle. Therefore the angle limiter can be set in arbitrary positions; during these measurements we use 4 specific positions: forward ($\varphi_0 = 0°$, $\varphi = 315–45°$), upward ($\varphi_0 = 90°$, $\varphi = 45–135°$), backward ($\varphi_0 = 180°$, $\varphi = 135–225°$), and downward ($\varphi_0 = 270°$, $\varphi = 225–315°$). For example, Fig. 1 shows the "forward" position of the angle selector. (In the case of spectrometer B, half of the entrance cone – the "forward" and "backward" quarters – are always closed). The ϑ scattering angle (the angle of the scattered or emitted electrons with respect to the primary beam) can be calculated from the angles α and φ:

$$\cos\vartheta = \sin\alpha\ \cos\varphi \tag{3}$$

as it simply can be read of Fig. 2. Based on this equation the following scattering angular ranges can be obtained: in case of medium entrance angle ($\alpha_0 = 43.5°$) for the forward sector 46.5—60.9°, for the upward and downward sectors 60.9—119.1°, and for the backward sectors 119.1—133.5°. In case we use the entire entrance angular range ($\alpha = 41–46°$), then the scattering angular ranges expand according to the following: forward sector 44—62.4°, the upward and downward sectors 59.4—120.6°, and the backward sectors 117.6—136°. Altogether, it can be said that the scattering angular ranges of the forward and backward sectors are much smaller ($\Delta\vartheta = 14.4°(18.4°)$) than the upward and downward sectors ($\Delta\vartheta = 58.2°(61.2°)$).

3. The structure of the autoionizing spectra of He

This work is based on measurements that were performed on the most important autoionizing states of helium. These $2s^2(^1S)$, $2s2p(^3P)$, $2p^2(^1D)$ and $2s2p(^1P)$ doubly excited states at excitation energies (E_R) 57.83 eV, 58.31 eV, 59.91 eV and 60.14 eV have been widely studied, even by the $(e,2e)$ method [8–15]. All these states decay to the same He^+1s^{-1} final state with $E_F = 24.59$ eV, hence the energies of the ejected autoionizing electrons ($E_a = E_R - E_F$) are 33.24 eV, 33.72 eV, 35.32 eV, and